

University of Nebraska - Lincoln

DigitalCommons@University of Nebraska - Lincoln

Anthony F. Starace Publications

Research Papers in Physics and Astronomy

1-21-2009

Analytic formulae for high harmonic generation

M. V. Frolov

Voronezh State University, Russia

N. L. Manakov

Voronezh State University, manakov@phys.vsu.ru

T. S. Sarantseva

Voronezh State University, Russia

Anthony F. Starace

University of Nebraska-Lincoln, astarace1@unl.edu

Follow this and additional works at: <https://digitalcommons.unl.edu/physicsstarace>



Part of the [Physics Commons](#)

Frolov, M. V.; Manakov, N. L.; Sarantseva, T. S.; and Starace, Anthony F., "Analytic formulae for high harmonic generation" (2009). *Anthony F. Starace Publications*. 165.

<https://digitalcommons.unl.edu/physicsstarace/165>

This Article is brought to you for free and open access by the Research Papers in Physics and Astronomy at DigitalCommons@University of Nebraska - Lincoln. It has been accepted for inclusion in Anthony F. Starace Publications by an authorized administrator of DigitalCommons@University of Nebraska - Lincoln.

Analytic formulae for high harmonic generation

M. V. Frolov,¹ N. L. Manakov,¹ T. S. Sarantseva,¹ and Anthony F. Starace²

¹ Department of Physics, Voronezh State University, Voronezh 394006, Russia

² Department of Physics and Astronomy, University of Nebraska-Lincoln, Lincoln, NE 68588-0111, USA

Abstract

Analytic formulae describing harmonic generation by a weakly bound electron are derived quantum mechanically in the tunneling limit. The formulae confirm the classical three-step model and provide an analytic explanation for oscillatory structures on the harmonic generation plateau.

1. Introduction

Exactly solvable models play a key role in understanding intense laser-atom phenomena. Especially attractive are those for which the final results have a simple analytic form, thereby providing the explicit dependence of experimentally measurable quantities on key parameters. The Keldysh formula for tunnelling ionization [1] is one such example. However, no such simple analytic formula exists for high-order harmonic generation (HHG), which is a more complex process. In particular, ionization represents only the initial step of the commonly accepted three-step scenario [2–4]. Semi-analytical quantum analyses of the HHG process that confirm this scenario are based primarily upon two alternative approaches: (i) the use of some version of the strong field approximation, including quasiclassical analyses in terms of electron trajectories (or quantum orbits) (cf. [5] for a review); or (ii) the use of some exactly solvable quantum model for the HHG problem. One such model (cf. [6, 7]) is based upon the exact solution of the time-dependent Schrödinger equation for an electron in both a zero-range potential (ZRP) and a strong laser field [8]; another, more general model (cf. [9]) is based on the time-dependent effective range (TDER) theory [10], within which the ZRP model is a special case (for bound states and an effective range parameter of zero). Among other semi-analytical HHG studies, we note the quantum analysis of [11], which supports the three-step scenario using a quasiclassical approach. Although Coulomb effects are usually neglected in semi-analytical analyses, such short-range potential model results in many instances exhibit good qualitative agreement with numerical results for neutral atoms [5, 12]. However, all semi-analytical HHG the-

ories (even the most simplified) require in a final step the numerical evaluation of one or more complicated temporal integrals.

An important extension of the three-step HHG scenario consists of the *ad hoc* factorization of the rate for generating the N th harmonic, $\mathcal{R}(E_\Omega)$ (where $E_\Omega = \hbar\Omega = N\hbar\omega$),

$$\mathcal{R}(E_\Omega) = W(E)\sigma^{(i)}(E), \quad E = E_\Omega - |E_0|, \quad (1)$$

in terms of the photorecombination cross section, $\sigma^{(i)}(E)$, of an active electron having energy $E = E_\Omega - |E_0|$ (where E_0 is its initial bound state energy) and an “electron wave packet,” $W(E)$, corresponding to the first two steps of the three-step scenario (i.e., ionization and propagation). The parametrization (1) was proposed in 2004 [13] for tomographic imaging of molecular orbitals (using the Born approximation result for $\sigma^{(i)}(E)$) and has recently been the subject of numerous detailed studies [14–17]. Although these recent studies support the factorization (1) and show that the energy dependence of the “electron wave packet” $W(E)$ is largely independent of the target atom (based upon both experimental measurements and numerical solutions of the time-dependent Schrödinger equation for a single active electron), the analytic structure of the function $W(E)$ remains a “black box.” Hence an analytic justification for the parametrization (1) as well as an explicit form for $W(E)$ is very desirable, even for an atomic system that may be regarded as a special case.

In this paper we derive surprisingly simple analytic formulae (involving a single Airy function) for the amplitudes and rates of harmonics generated by an electron bound in a short-range potential that provide excellent agreement with exact TDER results over the high energy part of the HHG plateau (and beyond). These results provide a quan-

tum justification for the classical three-step HHG scenario as well as a correction to the well-known classical law for the position of the HHG plateau cutoff. They also confirm the parametrization (1), show the insensitivity of $W(E)$ to the orbital symmetry (i.e., the angular momentum) of the bound electron wavefunction, and provide clear explanations for various qualitative features of HHG spectra, such as (i) the dependence of the oscillatory patterns of HHG rates in the plateau region on the harmonic number N , (ii) the dependence of the oscillatory patterns of the rate for the N th harmonic on the laser parameters and (iii) the dependence of the rates on the orbital angular momentum, l , of the bound electron.

2. Theory

We consider a single active electron in a bound state $\psi_{\kappa lm}(\mathbf{r}) = R_{\kappa l}(r)Y_{lm}(\hat{\mathbf{r}})$, having angular momentum l and energy $E_0 = -(\hbar\kappa)^2/(2m)$, that interacts with a monochromatic laser electric field $\mathbf{F}(t) = \hat{\mathbf{z}} F \cos \omega t$, where F and ω are the field amplitude and frequency. Employing our recently developed *ab initio* quantum formulation for the HHG amplitude [18], the rate $\mathcal{R}^{(l)}(E_\Omega)$ is

$$\mathcal{R}^{(l)}(E_\Omega) = \frac{1}{2l+1} \frac{E_\Omega^3}{8\pi\hbar^4 c^3} \sum_m |\chi_N^{(m)}(F, \omega)|^2. \quad (2)$$

Here $\chi_N^{(m)}(F, \omega)$ is the HHG amplitude, which can be expressed in terms of the complex quasienergy of the electron in both the laser field $\mathbf{F}(t)$ and a weak (probe) field of frequency Ω . Within the framework of TDER theory (i.e. assuming an electron bound by short-range forces that has only a single bound state, $\psi_{\kappa lm}(\mathbf{r})$, dynamically interacting with the three-dimensional continuum), the explicit form of $\chi_N^{(m)}(F, \omega)$ is given in [9]. Moreover, the analysis in [9] shows that (i) the partial rate with zero projection m of the angular momentum in the direction of linear laser polarization gives the dominant contribution to the rate (2) and (ii) for low frequencies, the exact TDER results are in perfect agreement with those in the quasiclassical approximation.

The subject of this paper is an analytical evaluation of the quasiclassical result for the HHG amplitude, to which our exact quantum TDER result [9] reduces in the limit $\hbar\omega \ll |E_0|$. To simplify the notation, in the rest of this theoretical section we use scaled units (su), in which energies and ω are measured in units of $|E_0|$ and $|E_0|/\hbar$ respectively and laser field amplitudes, F , are given in units of $F_0 = (2m|E_0|^3)^{1/2}/|e|\hbar$. In these units, our quasiclassical result for $\chi_N(F, \omega)$ for the cases of initial s ($l=0$) and p ($l=1$, $m=0$) states can be presented as follows [9]:

$$\chi_N(F, \omega) = \sum_n \mathcal{Z}_{l,n} \int_{-T/2}^{T/2} \frac{e^{i[\Omega t + S(P_n, t_0) - S(P_n, t)]}}{\cos \omega t_0 - \cos \omega t} \times \frac{(P_n - p_t)^{l+1} - \delta_{l,1}}{[(P_n - p_t)^2 + 1]^2} dt, \quad T = 2\pi/\omega, \quad (3)$$

where $p_t = -(F/\omega) \sin \omega t$, $P_n = (n\omega - 1 - u_p)^{1/2}$, $u_p = F^2/(2\omega^2) = (e^2 F^2)/(4m\omega^2)$ (in absolute units) is the ponderomotive energy, and the classical action, $S(P_n, t)$, and the amplitude,

$\mathcal{Z}_{l,n}$, are defined by

$$S(P_n, t) = \int^t [(P_n - p_{t'})^2 + 1] dt', \quad (4)$$

$$\mathcal{Z}_{l,n} = i \frac{3^l C_{\kappa l}^2 \omega^4}{2^l \pi^2 F} \sqrt{\frac{2\pi i}{S''(P_n, t_0)}},$$

where $C_{\kappa l}$ is the coefficient in the asymptotic form (in absolute units) of $\psi_{\kappa lm}(\mathbf{r}) \approx C_{\kappa l} r^{-1} \exp(-\kappa r) Y_{lm}(\hat{\mathbf{r}})$ for $r \gg \kappa^{-1}$. The time t_0 in (3) and (4) is the root of the saddle point equation, $(P_n - p_{t_0})^2 + 1 = 0$, having positive imaginary part and the smallest value of $\text{Re } t_0$. As discussed in [9], for s states our result (3) coincides with that obtained in [11] by an alternative quantum analysis of the HHG amplitude, represented in terms of the Fourier coefficients of a field-induced dipole moment.

In order to evaluate expression (3), we first replace the sum over n by an integral over the active electron's momentum, p , using the following substitutions:

$$P_n \rightarrow p, \quad \sum_n f(P_n) \rightarrow \frac{2}{\omega} \int_0^\infty f(p) p dp. \quad (5)$$

Introducing the new variables, $k = \gamma p$ and $\tau = \omega t$, expression (3) has the form

$$\chi_N(F, \omega) = \mathcal{C} \int_0^\infty k dk \int_{-\pi}^\pi d\tau \frac{e^{i\Phi(k, \tau)}}{\sqrt{\cos \tau_0}} \times \frac{(k + \sin \tau)^{l+1} - \gamma^2 \delta_{l,1}}{(\cos \tau - \cos \tau_0)[\gamma^{-2}(k + \sin \tau)^2 + 1]^2}, \quad (6)$$

where $\gamma = \omega/F = [(2m|E_0|)^{1/2}\omega]/(|e|F)$ (in absolute units) is the Keldysh parameter,

$$\mathcal{C} = 2 \left(\frac{3}{2}\right)^l \frac{C_{\kappa l}^2 F^{l+3/2}}{\pi^{3/2} \omega^{l+1}}, \quad \tau_0 = \omega t_0, \quad (7)$$

$$\Phi(k, \tau) = \frac{\Omega}{\omega} \tau + \frac{1}{\omega} \int_\tau^{\tau_0} [\gamma^{-2}(k + \sin \xi)^2 + 1] d\xi.$$

In terms of γ , τ_0 satisfies the equation, $(k + \sin \tau_0)^2 + \gamma^2 = 0$, or

$$\sin \tau_0 = -i\gamma - k. \quad (8)$$

For later use, we note also the following results for the derivatives $\partial\tau_0/\partial\gamma$ and $\partial\tau_0/\partial k$,

$$\partial\tau_0/\partial\gamma = -i/\cos \tau_0, \quad \partial\tau_0/\partial k = -1/\cos \tau_0. \quad (9)$$

For $\gamma \rightarrow 0$ (i.e. in the strong field, or tunneling, limit), both integrals in (6) are highly oscillatory, so that saddle point methods may be used to evaluate them. Saddle points for the integral over k are given by the equation, $\partial(k, \tau)/\partial k = 0$, or

$$k = (\cos \tau - \cos \tau_0)/(\tau - \tau_0), \quad (10)$$

while those for the integral over τ in (6) satisfy the equation, $\partial\Phi(k, \tau)/\partial\tau = 0$, or

$$\Omega - 1 = \gamma^{-2}(k + \sin \tau)^2. \quad (11)$$

We consider first the exact saddle-point equations (8), (10), and (11) to lowest order in γ . According to (8), $\tau_0 \approx \tilde{\tau}_0$ for this case, where $\sin \tilde{\tau}_0 = -k$, while k is given by (10) after

substituting $\tau_0 \rightarrow \tilde{\tau}_0$. We then eliminate k by substituting $k = -\sin \tilde{\tau}_0$ in (10) and (11) to obtain the following system of two coupled equations,

$$-\sin \tilde{\tau}_0 = (\cos \tau - \cos \tilde{\tau}_0) / (\tau - \tilde{\tau}_0), \quad (12)$$

$$\Omega - 1 = \gamma^{-2} (\sin \tau - \sin \tilde{\tau}_0)^2, \quad (13)$$

for two characteristic times (in units of ω^{-1}), $\tilde{\tau}_0$ and τ , corresponding (in the three-step HHG model) to the moments of ionization and recombination of the active electron. Equations (12) and (13) coincide with the classical equations for a free electron in the laser field, moving along a closed trajectory: equation (12) determines the time τ at which the electron, starting at the time $\tilde{\tau}_0$ from some point \mathbf{r} , returns to the same point \mathbf{r} , while the right-hand side of (13) gives the energy, $\mathcal{E}_{\text{cl}}(\tau)$, gained by the electron from the laser field over the time interval $(\tau - \tilde{\tau}_0)$ [6]. (Note that the appearance of classical features in our quantum analysis of the HHG amplitude is not surprising since the classical equations (12) and (13) arise from treating in (7) the classical action,

$$S(k, \tau_0) = \frac{1}{\omega} \int_{\tau_0}^{\tau_0} [(k + \sin \xi)^2 \gamma^{-2} + 1] d\xi, \quad (14)$$

for real $t_0 (= \tilde{\tau}_0)$.) An analysis of the classical equations (12) and (13) in section V of [6] shows that the function $\mathcal{E}_{\text{cl}}(\tau) = \gamma^{-2} (\sin \tau - \sin \tilde{\tau}_0)^2$ has the famous maximum,

$$\mathcal{E}_{\text{cl}}^{\text{max}} \equiv \max \mathcal{E}_{\text{cl}}(\tau) = \gamma^{-2} \sin^2(\tau_{\text{cl}}/2) \approx 3.173 u_p, \quad (15)$$

at $\tau = \tilde{\tau}^{(\text{cl})} = \tilde{\tau}_{\text{cl}}/2 - \pi/4$ and $\tilde{\tau}_0 = \tilde{\tau}_0^{(\text{cl})} = -\tau_{\text{cl}}/2 - \pi/4$, where $\tau_{\text{cl}} = \tilde{\tau}^{(\text{cl})} - \tilde{\tau}_0^{(\text{cl})} \approx 4.086$ is the return time along a closed trajectory.

The zeroth-order (in γ) approximation for k ($k = -\sin \tilde{\tau}_0$) is not sufficiently accurate for the saddle-point evaluation of the integral over k in (6). We thus expand the right-hand side of (10) up to terms $\sim \gamma^2$, using (8) and (9), to obtain

$$k \approx \tilde{k} = -\sin \tilde{\tau}_0 - \frac{\gamma^2}{2(\tau - \tilde{\tau}_0) \cos \tilde{\tau}_0}. \quad (16)$$

Substituting $k \rightarrow \tilde{k}$ into $\Phi(k, \tau)$ (and $k \rightarrow -\sin \tilde{\tau}_0$ otherwise) and using the lowest-order (in γ) expression for the second derivative of (k, τ) ,

$$\frac{\partial^2 \Phi(k, \tau)}{\partial k^2} \approx -\frac{2(\tau - \tilde{\tau}_0)}{\gamma^2 \omega}, \quad (17)$$

the saddle-point integration over k in (6) gives

$$\begin{aligned} \chi_N(F, \omega) &= \gamma \sqrt{-\pi i \omega C} \int_{-\pi}^{\pi} d\tau \frac{e^{i\Phi(\tilde{k}, \tau)}}{\sqrt{\cos \tilde{\tau}_0}} \\ &\times \frac{(\sin \tau - \sin \tilde{\tau}_0)^{l+1} - \gamma^2 \delta_{l,1}}{(\tau - \tilde{\tau}_0)^{3/2} [\gamma^{-2} (\sin \tau - \sin \tilde{\tau}_0)^2 + 1]^2}. \end{aligned} \quad (18)$$

The integration over τ in (18) requires a more detailed analysis of $\Phi(k, \tau)$, taking into account high-order corrections in γ . Substituting $k \rightarrow \tilde{k}$ into $\gamma^2 \mathcal{E}(\tau) = (k + \sin \tau)^2$ and expanding the result in γ up to terms $\sim \gamma^2$, we obtain

$$\mathcal{E}(\tau) \approx \mathcal{E}_{\text{cl}}(\tau) + \delta \mathcal{E}(\tau), \quad \delta \mathcal{E}(\tau) = -\frac{\sin \tau - \sin \tilde{\tau}_0}{\cos \tilde{\tau}_0 (\tau - \tilde{\tau}_0)}. \quad (19)$$

The maximum value of $\mathcal{E}(\tau)$ can be found by setting $\tau = \tilde{\tau}^{(\text{cl})}$ and $\tilde{\tau}_0 = \tilde{\tau}_0^{(\text{cl})}$ in (19)

$$\mathcal{E}_{\text{max}} \equiv \max \mathcal{E}(\tau) \approx \mathcal{E}_{\text{cl}}^{\text{max}} + \Delta, \quad (20)$$

where Δ is given by $\delta \mathcal{E}(\tau)$ in (19) at $\tau = \tilde{\tau}^{(\text{cl})}$, $\tilde{\tau}_0 = \tilde{\tau}_0^{(\text{cl})}$ and can be represented as

$$\Delta = -(\partial \tilde{\tau}_0 / \partial \tau) |_{\tau = \tilde{\tau}^{(\text{cl})}} \approx 0.324. \quad (21)$$

(Note that the quantum correction $\Delta = 0.32$ to $\mathcal{E}_{\text{cl}}^{\text{max}}$ in the limit $\gamma \rightarrow 0$ was obtained also in [4] within the saddle-point approximation. In addition, there it was shown that this correction slowly decreases with decreasing intensity, e.g., $\Delta \simeq 0.27$ at $\gamma = 1$.)

Near its maximum (at $\tau = \tau_{\text{max}} \approx \tilde{\tau}^{(\text{cl})}$), the energy $\mathcal{E}(\tau)$ is approximated as

$$\mathcal{E}(\tau) \approx \tilde{\mathcal{E}}(\tau) = \mathcal{E}_{\text{max}} - \delta (\tau - \tilde{\tau}^{(\text{cl})})^2 / \gamma^2, \quad (22)$$

where the dispersion parameter δ (to lowest order in γ) is

$$\delta = -(1/2) \gamma^2 \mathcal{E}_{\text{cl}}''(\tilde{\tau}^{(\text{cl})}) \approx 1.072. \quad (23)$$

(The quantum corrections $\sim \gamma^2$ to τ_{max} and δ and the correction $\sim \gamma^2$ to Δ also have a closed analytic form; however, because they give negligible contributions to the final results, we do not present them here.) Using (22) and a relation following from (7),

$$\frac{\partial \Phi(\tilde{k}, \tau)}{\partial \tau} = \frac{1}{\omega} [\Omega - 1 - \mathcal{E}(\tau)], \quad (24)$$

the function $\Phi(\tilde{k}, \tau)$ in (7) is approximated by a cubic polynomial in τ

$$\begin{aligned} \Phi(\tilde{k}, \tau) &\approx \Phi_0 + \frac{\Omega - 1 - \mathcal{E}_{\text{max}}}{\omega} (\tau - \tilde{\tau}^{(\text{cl})}) \\ &+ \frac{\delta}{3\gamma^2 \omega} (\tau - \tilde{\tau}^{(\text{cl})})^3. \end{aligned} \quad (25)$$

The τ -independent factor Φ_0 is related to $\Phi(\tilde{k}, \tau_0)$ (cf. (14)): $\Phi_0 = (\Omega/\omega) \tilde{\tau}^{(\text{cl})} + S(\tilde{k}, \tau_0) - S(\tilde{k}, \tilde{\tau}^{(\text{cl})})$. Taking into account the correction $\sim \gamma$ to $\tilde{\tau}_0$ using (8) and (9) ($\tau_0 = \tilde{\tau}_0 - i\gamma/\cos \tilde{\tau}_0$, where $\cos \tilde{\tau}_0 \approx \cos \tilde{\tau}_0^{(\text{cl})} = -0.95 \dots$), Φ_0 may be presented as

$$\begin{aligned} \Phi_0 &\approx S(-\sin \tilde{\tau}_0^{(\text{cl})}, \tilde{\tau}_0^{(\text{cl})}) - S(-\sin \tilde{\tau}_0^{(\text{cl})}, \tilde{\tau}^{(\text{cl})}) \\ &+ \frac{\Omega}{\omega} \tilde{\tau}^{(\text{cl})} + i \frac{2}{3\tilde{F}}, \quad \tilde{F} = F |\cos \tilde{\tau}_0^{(\text{cl})}|. \end{aligned} \quad (26)$$

Finally, using (25) and (26) and substituting $\tilde{\tau}_0 \rightarrow \tilde{\tau}_0^{(\text{cl})}$, $(\tau - \tilde{\tau}_0) \rightarrow \tau_{\text{cl}} (\sin \tau - \sin \tilde{\tau}_0) \rightarrow \gamma (\Omega - 1)^{1/2}$ in the integrand of (18), the integral over τ can be expressed in terms of the Airy function, $\text{Ai}(x)$, so that χ_N takes the form

$$\begin{aligned} \chi_N(F, \omega) &= e^{i(\text{Re} \Phi_0 - \pi/4)} \frac{3^l C_{\kappa l}^2 \omega^{5/2}}{2^{l-2} \tau_{\text{cl}}^{3/2} \Omega^2 (\sqrt{\delta F})^{2/3} \sqrt{\tilde{F}}} \\ &\times e^{-2/(3\tilde{F})} (\Omega - 1 - l)^{\frac{l+1}{2}} \text{Ai} \left(\frac{\Omega - 1 - \mathcal{E}_{\text{max}}}{(\sqrt{\delta F})^{2/3}} \right). \end{aligned} \quad (27)$$

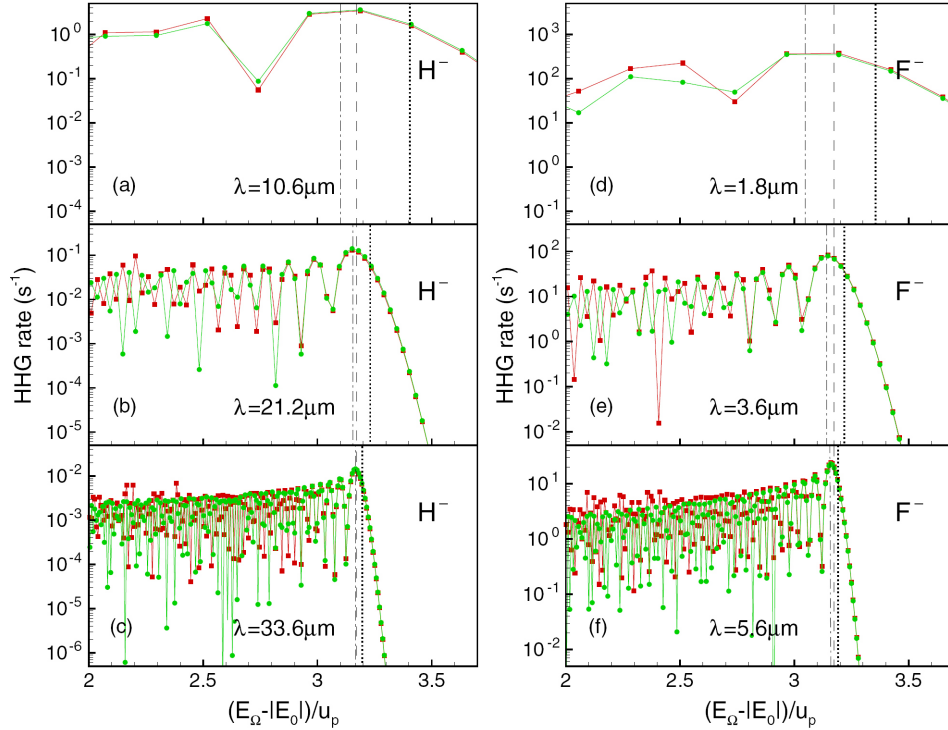


Figure 1. HHG spectra (with harmonic energies $E_{\Omega} \geq (|E_0| + 2.0u_p)$) at three different wavelengths for H^- at $I = 10^{11} \text{ W cm}^{-2}$ (left) and F^- at $I = 2 \times 10^{13} \text{ W cm}^{-2}$ (right). Squares (red): exact TDER results; circles (green): analytic result (28). Vertical dash-dotted, dashed, and dotted lines show the HHG cutoff positions according to (30), (31), and (32) respectively.

3. Analytic three-step formula for HHG rates and discussion

Converting χ_N in (27) from scaled to absolute units and substituting the result into (2), the HHG rate takes the following analytic form:

$$\mathcal{R}^{(l)}(E_{\Omega}) = \frac{|E_0|^2}{E_{\text{at}}\hbar} \frac{A_{\kappa l}}{N} \left(\frac{\hbar\omega}{|E_0|} \right)^4 \left(\frac{F_0}{\sqrt{\delta}F} \right)^{4/3} \frac{F_0}{\bar{F}} \times e^{-4F_0/(3\bar{F})} (E/|E_0| - l)^{l+1} \text{Ai}^2(\xi), \quad (28)$$

where

$$E = E_{\Omega} - |E_0|, \quad \xi = \frac{E - \mathcal{E}_{\text{max}}}{|E_0|(\sqrt{\delta}F/F_0)^{2/3}},$$

$$A_{\kappa l} = \frac{\alpha^3}{\pi} \left(\frac{3}{4} \right)^l \frac{C_{\kappa l}^4}{\kappa^2 \tau_{\text{cl}}^3}, \quad E_{\text{at}} = \frac{me^4}{\hbar^2} \simeq 27.21 \text{ eV},$$

$$\alpha \simeq \frac{1}{137}. \quad (29)$$

Figure 1 compares results of the analytic formula (28) with exact numerical evaluation of the amplitude (3) for the cases of HHG in the negative ions H^- and F^- . One sees that for harmonic energies at the high energy end of the HHG plateau, as well as beyond the plateau cutoff, the agreement of the analytic and the exact numerical results is excellent. Note that (28) correctly predicts the rate for the cutoff harmonics even for the case when γ ($= 0.60$ for H^- and 0.53 for F^-) is not small. This fact is similar to that for the Keldysh tunneling rate, which also was derived for small γ , but which in practice has been found to provide reasonable rates up to $\gamma < 1$.

The analytic formulae (27) and (28) allow one to obtain a number of general results, which we discuss in turn. First, since $\text{Ai}(\xi)$ decreases rapidly for positive ξ and oscillates for $\xi < 0$, the plateau cutoff, E_{Ω}^{max} , follows by equating the argument of $\text{Ai}(\xi)$ in (28) to the position ξ_1 (≈ -1.019) of the first maximum of $\text{Ai}(\xi)$ for $\xi < 0$

$$E_{\Omega}^{\text{max}} = \mathcal{E}_{\text{cl}}^{\text{max}} + [1 + \Delta - |\xi_1| \delta^{1/3} (F/F_0)^{2/3}] |E_0|, \quad (30)$$

where $|\xi_1| \delta^{1/3} \approx 1.08$. For $\Delta = \delta = 0$, (30) reduces to the classical cutoff law [2, 3, 6],

$$E_{\Omega}^{\text{max}} = \mathcal{E}_{\text{cl}}^{\text{max}} + |E_0|, \quad (31)$$

while if one retains only the correction Δ , one obtains the cutoff law predicted in [4]

$$E_{\Omega}^{\text{max}} = \mathcal{E}_{\text{cl}}^{\text{max}} + (1 + \Delta) |E_0|. \quad (32)$$

The field amplitude (F_{cr}) at which the corrections $\sim \delta$ and Δ in (30) approximately compensate each other is $F_{\text{cr}} \approx 0.17$ su or $F_{\text{cr}} \approx 0.24 (|E_0|/E_{\text{at}})^{3/2} F_{\text{at}}$ in absolute units, where $F_{\text{at}} = m^2 |e|^{5/\hbar^4} \simeq 5.14 \times 10^9 \text{ V cm}^{-1}$. For H^- and F^- , F_{cr} corresponds to intensities of about 4×10^{10} and $4 \times 10^{12} \text{ W cm}^{-2}$, respectively. This approximate compensation explains why the classical result (31) is in good agreement with our more accurate estimate (30) and with the exact results in Figure 1, whereas accounting only for the correction Δ systematically overestimates the cutoff position. (For rare gas atoms, we estimate that this compensation occurs in the range 10^{14} – $10^{15} \text{ W cm}^{-2}$.)

The positions of the maxima and minima in the oscillatory behavior of $\mathcal{R}^{(l)}(E_{\Omega})$ shown in Figure 1 for $E_{\Omega} < E_{\Omega}^{\text{max}}$

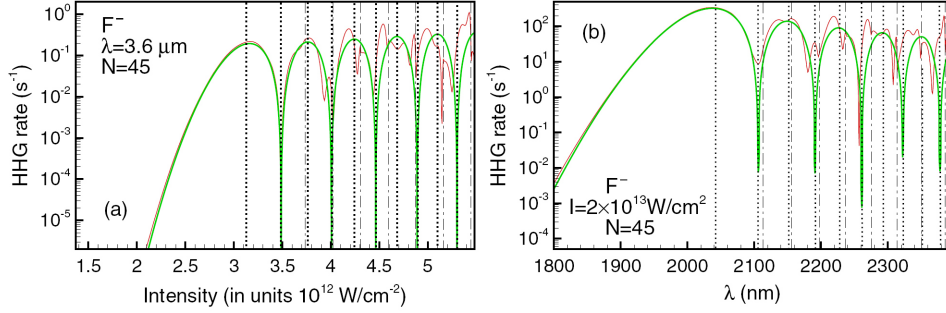


Figure 2. Oscillatory patterns in the intensity (a) and wavelength (b) dependences of the rate for the 45th harmonic in F^- . Thin (red) line: exact TDER results; thick (green) line: analytic result (28). Vertical dotted lines: positions of the maxima/minima according to (34); dot-dashed lines: positions of the n -photon detachment thresholds (given by the condition: $|E_0| + u_p = n\hbar\omega$), where $20 \leq n \leq 27$ in panel (a), and $23 \leq n \leq 29$ in panel (b). The HHG plateau cutoff is given by the leftmost vertical dotted line in each panel.

coincide with the positions (ξ_n) of the maxima/minima of the Airy function in (28) (cf. (30)). For $n \geq 2$, these positions are well approximated by equating to $\pi n/2$ the argument of the sine function in the asymptotic form of $\text{Ai}(-|\xi|)$ for large $|\xi|$,

$$\text{Ai}(-|\xi|) \sim |\xi|^{-1/4} \sin\left(\frac{2}{3}|\xi|^{3/2} + \frac{\pi}{4}\right). \quad (33)$$

The minima (maxima) of $\mathcal{R}^{(l)}(E_\Omega)$, at the energies $(E_\Omega)_{\text{max}/\text{min}}$ correspond to even (odd) n in the relation

$$\xi = \xi_n = -0.25[3\pi(2n-1)]^{2/3}, \quad n \geq 2, \quad (34)$$

where ξ is given by (29). The energies $(E_\Omega)_{\text{max}/\text{min}}$ are given by equation (30) upon making there the following two replacements: $E_\Omega^{\text{max}} \rightarrow (E_\Omega)_{\text{max}/\text{min}}$ and $\xi_1 \rightarrow \xi_n$. (Note that the oscillatory behavior of $\mathcal{R}^{(l)}(E_\Omega)$ was described in [19] as the result of interference between two effective (complex-valued) electron trajectories.)

Condition (34) also describes the interference oscillations in the intensity and frequency dependences of the rate for a fixed (N th) harmonic. In this case, condition (34) gives a transcendental equation for the intensities or frequencies corresponding to minima and maxima of these oscillations. Such oscillation patterns in the intensity dependence of HHG rates have been discussed in [4, 19, 20] (see also a recent experiment [21]) and interpreted in [19, 20] in terms of the interference between two electron trajectories. In Figure 2 we present results for the 45th harmonic in F^- . One sees that (34) correctly describes the exact results in the cut-off region, while with increasing intensity or wavelength (when the position of the N th harmonic moves to the middle part of the plateau) threshold phenomena corresponding to the closing/opening of the lowest-order multiphoton detachment channels (which were not taken into account in our derivations of $\mathcal{R}^{(l)}(E_\Omega)$ due to the substitution (5)) significantly affect the results (see [12, 22] for details).

The result (28) also explains the l -dependence of HHG rates, which originates completely from the recombination step of the three-step HHG model. Indeed, the recombination cross section from the free electron continuum state, $\psi_p(\mathbf{r}) = \exp(i\mathbf{p} \cdot \mathbf{r}/\hbar)$ with momentum \mathbf{p} directed along the

laser polarization (with $p = [2m(E_\Omega - |E_0|)]^{1/2}$) to the s and p bound states $\psi_{klm}(\mathbf{r})$, whose radial wavefunctions outside the short-range potential well are given by spherical Hankel functions $h_l^{(1)}(ikr)$, is

$$\begin{aligned} \sigma^{(r)}(E) &= \frac{\Omega^3}{2\pi c^3} \frac{\hbar}{a_0 p} |\langle \psi_p | z | \psi_{kl,m=0} \rangle|^2 \\ &= \alpha^3 C_{kl}^2 \kappa^{-1} \left(\frac{3}{4}\right)^l \frac{(E/|E_0| - l)^{l+1}}{\sqrt{E/|E_0|}(E/|E_0| + 1)} a_0^2, \end{aligned} \quad (35)$$

where a_0 is the Bohr radius. The l -dependent term in (35) coincides precisely with that in the HHG rate (28), which corresponds, therefore, to the recombination factor in the three-step HHG scenario and justifies the parametrization of $\mathcal{R}^{(l)}(E_\Omega)$ in the form (1). Note that the rate (28) involves the Born approximation result (35) for $\sigma^{(r)}(E)$ because our quasiclassical result (3) was obtained in an approximation that takes minimal account of the electron-atom interaction [9], i.e., only for the initial bound state wavefunction, as in the Keldysh approximation [1] for tunnel ionization.

The F -dependent exponential in (28) is related to the rate of tunnel ionization in an effective static electric field of strength $\tilde{F} = F |\cos \tilde{\tau}_0^{(\text{cl})}|$, which corresponds to $\mathbf{F}(t)$ at the moment of ionization, $\tau = \tilde{\tau}_0^{(\text{cl})}$. (This is a consequence of our approximation $\gamma \ll 1$, which is equivalent to the quasistatic limit.) Our key results (27), (28) factorize into a product of three terms corresponding to the three-step model, thus providing a convincing quantum justification for this model. The most interesting one is the “free-propagation” factor, involving the Airy function and describing all interference (oscillation) effects. To the best of our knowledge, our analysis of the HHG process is the first one in which this factor is presented explicitly, in closed analytic form. In particular, our result shows that the energy dependence of the “electron wave packet” in (1) is given by $W(E) \sim E^{1/2} \text{Ai}^2(\xi)$. The appearance of Airy functions is typical of static-electric-field-mediated photodetachment (cf. [23], in which they describe the interference between two electron trajectories in a static electric field). In our case, the electron energy $\tilde{\mathcal{E}}(\tau)$ in (22) is approximated by a quadratic function near $\tau = \tilde{\tau}^{(\text{cl})}$, so that the classical electron momen-

tum becomes a linear function of time (as in a static electric field). The interference may be attributed to two (“short” and “long”) closed electron trajectories, that start at $\tau = \tilde{\tau}_0^{(cl)}$ and end at $\tau = \tilde{\tau}^{(cl)} \mp \gamma[(\mathcal{E}_{\max} - E_{\Omega} + |E_0|)/(\delta|E_0|)]^{1/2}$. These trajectories originate from the single (“degenerate”) trajectory corresponding to the cutoff energy (i.e. $\tau = \tilde{\tau}_0^{(cl)}$), which splits into two different trajectories when the energy slightly decreases from the cutoff, according to (22).

4. Conclusions

In conclusion, for an electron bound by a short-range potential, $U(r)$, we have presented an accurate quantum derivation of closed form analytic formulae for HHG amplitudes and rates having the same level of transparency and simplicity as the Keldysh result for tunnel ionization. These formulae justify both the classical three-step HHG scenario and the *ad hoc* parametrization (1). They also describe all key features of HHG spectra. Although the TDER theory (which is independent of the shape of $U(r)$) is quantitatively reliable only for negative ions, the structure of our key (three-step) results (27), (28) leads one to expect that the “free-propagation” factor there has a universal character, describing the motion of a detached or ionized electron in a laser-modified continuum, while the effects of the potential $U(r)$ are most significant for the “bound state” (ionization and recombination) factors. (This expectation is supported also by the fact that the “electron wave packet” in the parametrization (1) is essentially independent of the atomic species, as discussed in [13–17].) For quantitative predictions of HHG rates in atoms, a generalization of our derivations in this paper is necessary in order to incorporate properly the Coulomb ionization and recombination factors into (28). This generalization, using hydrogen atom wavefunctions for $\psi_{\kappa lm}(\mathbf{r})$, is now in progress.

Acknowledgments

This work was supported in part by RFBR grant no 07-0200574 and by NSF grant no. PHY-0601196. TSS acknowledges the support of the “Dynasty” Foundation.

References

- [1] Keldysh L V 1964 *Zh. Eksp. Teor. Fiz.* **47** 1945
Keldysh L V 1965 *Sov. Phys.-JETP* **20** 1307
- [2] Schafer K J, Yang B, DiMauro L F, and Kulander K C 1993 *Phys. Rev. Lett.* **70** 1599
- [3] Corkum P B 1993 *Phys. Rev. Lett.* **71** 1994
- [4] Lewenstein M, Balcou Ph, Ivanov M Yu, L’Huillier A, and Corkum P B 1994 *Phys. Rev. A* **49** 2117
- [5] Becker W, Grasbon F, Kopold R, Milošević D B, Paulus G G, and Walther H 2002 *Adv. At. Mol. Opt. Phys.* **49** 35
- [6] Becker W, Long S, and McIver J K 1994 *Phys. Rev. A* **50** 1540
- [7] Borca B, Starace A F, Flegel A V, Frolov M V, and Manakov N L 2002 *Phys. Rev. A* **65** 051402
- [8] Manakov N L and Fainshtein A G 1980 *Zh. Eksp. Teor. Fiz.* **79** 751
Manakov N L and Fainshtein A G 1980 *Sov. Phys.-JETP* **52** 382
- [9] Frolov M V, Flegel A V, Manakov N L, and Starace A F 2007 *Phys. Rev. A* **75** 063408
- [10] Frolov M V, Manakov N L, Pronin E A, and Starace A F 2003 *Phys. Rev. Lett.* **91** 053003
- [11] Kuchiev M Yu and Ostrovsky V N 1999 *J. Phys. B: At. Mol. Opt. Phys.* **32** L189
Kuchiev M Yu and Ostrovsky V N 1999 *Phys. Rev. A* **60** 3111
- [12] Frolov M V, Manakov N L, and Starace A F 2008 *Phys. Rev. Lett.* **100** 173001
- [13] Itatani J, Levesque J, Zeidler D, Niikura H, Pépin H, Kiefer J C, Corkum P B, and Villeneuve D M 2004 *Nature* **432** 867
- [14] Levesque J, Zeidler D, Marangos J P, Corkum P B, and Villeneuve D M 2007 *Phys. Rev. Lett.* **98** 183903
- [15] Morishita T, Le A T, Chen Z, and Lin C D 2008 *Phys. Rev. Lett.* **100** 013903
- [16] Le A T, Della Picca R, Fainstein P D, Telnov D A, Lein M and Lin C D 2008 *J. Phys. B: At. Mol. Opt. Phys.* **41** 081002
- [17] Le A T, Morishita T, and Lin C D 2008 *Phys. Rev. A* **78** 023814
- [18] Frolov M V, Flegel A V, Manakov N L and Starace A F 2007 *Phys. Rev. A* **75** 063407
- [19] Kuchiev M Yu and Ostrovsky V N 2001 *J. Phys. B: At. Mol. Opt. Phys.* **34** 405
- [20] Platonenko V T 2001 *Quantum Electron.* **31** 55
- [21] Zaïr A et al 2008 *Phys. Rev. Lett.* **100** 143902
- [22] Manakov N L and Frolov M V 2006 *Pis’ma ZETF* **83** 630
Manakov N L and Frolov M V 2006 *JETP Lett.* **83** 536
- [23] Fabrikant I I 1980 *Zh. Eksp. Teor. Fiz.* **79** 2070
Fabrikant I I 1980 *Sov. Phys.-JETP* **52** 1045